AJNR

Cerebral N-acetylaspartate is low in patients with multiple sclerosis and abnormal visual evoked potentials.

A C Heide, G H Kraft, J C Slimp, J C Gardner, S Posse, S Serafini, J D Bowen and T L Richards

AJNR Am J Neuroradiol 1998, 19 (6) 1047-1054
http://www.ajnr.org/content/19/6/1047

AJNR Am J Neuroradiol 19:1047–1054, June 1998

Cerebral *N*-Acetylaspartate Is Low in Patients with Multiple Sclerosis and Abnormal Visual Evoked Potentials

A. C. Heide, G. H. Kraft, J. C. Slimp, J. C. Gardner, S. Posse, S. Serafini, J. D. Bowen, and T. L. Richards

PURPOSE: **Our purpose was to compare cerebral proton MR metabolite changes in patients with multiple sclerosis (MS) and abnormal visual evoked potentials (VEPs) with those in MS patients with normal VEPs.**

METHODS: **Seventeen subjects with clinically definite MS were studied with VEPs and MR spectroscopic imaging. Proton MR metabolites were measured using a fast spectroscopic imaging technique called proton echo-planar spectroscopic imaging (PEPSI). Kurtzke's Expanded Disability Status Scale (EDSS) score was also ascertained for each subject to obtain a clinical rating. Twelve regions of interest within the visual pathway of the cerebrum were evaluated for levels of *N*-acetylaspartate (NAA), choline, creatine, and the presence or absence of MR-detectable lesions.**

RESULTS: **PEPSI NAA values (water-normalized, CSF-corrected) were significantly lower in MS subjects with abnormal VEPs than in subjects with normal VEPs. MR-detectable lesion fractions and EDSS scores were also significantly different between the two VEP groups, but NAA comparison had a *P* value 100 times less than either of these measures.**

CONCLUSION: **In patients with MS, NAA measurements in the optic pathways of the brain were sensitive to VEP abnormalities. NAA was more sensitive to VEP changes than were choline, creatine, MR-detectable lesions, and EDSS score.**

Multiple sclerosis (MS) is a demyelinating disease of the CNS associated with a series of immune-mediated events. The damage done to the CNS leaves the patient with deficits in motor, sensory, or cognitive functioning. The process of demyelination in MS has been evaluated by several techniques, including conventional MR imaging (1) and visual evoked potentials (VEPs) (2–7). Even though conventional MR imaging has been established as a reliable, objective technique to assist in diagnosing and following the progression of MS (1), it is limited to the observation of changes in water mobility. Evoked potential techniques can be used to observe changes in nerve conduction properties, but the exact site along the conduction pathway cannot be determined.

Using single-voxel MR spectroscopic techniques, several investigators have reported decreases in the chemical ratio of *N*-acetylaspartate (NAA)/creatine and increases in the chemical ratio of choline/creatine in the brains of patients with MS relative to control subjects (8–13). These chemical changes may occur within or outside of lesions detected by MR imaging. Single-voxel spectroscopic techniques are useful in measuring the chemical differences between MS patients and control subjects, but they do not give a spatial distribution of the metabolites.

Patients with MS often undergo evoked potential studies to determine if demyelination has affected the conduction of sensory potentials along white matter tracts. VEP techniques are useful in detecting lesions of the visual pathways (2, 3, 5–7, 14), but the exact site of the lesion is often difficult to locate because of limitations in the recording technique. The purpose of this study was to compare the proton metabolite changes in the brains of MS patients with abnormal VEPs against those in MS patients with normal VEPs by using proton echo-planar spectroscopic imaging

Received June 2, 1997; accepted after revision October 31.

Supported by grant R01 NS 30722 from the Neurologic Disorders and Stroke Division of the NIH.

Presented in part at the annual meeting of the American Society of Neuroradiology, Seattle, June 1996.

From the Departments Radiology (A.C.H., J.C.G., T.L.R.), Rehabilitation Medicine (G.H.K., J.C.S.), Speech and Hearing Sciences (S.S.), and Neurology (J.D.B.), University of Washington, Seattle; and the Institut fur Medizin, Forschungszentrum Julich GmbH, D-52425, Germany (S.P.).

Address reprint requests to Todd Richards, PhD, Department of Radiology, Box 356004, University of Washington Medical Center, Seattle, WA 98195.

(PEPSI) along with parallel measurements of MR-detectable lesions and a clinical disability rating.

Methods

Subjects

Seventeen subjects, nine women and eight men, with clinically definite MS supported by clinical and objective measurements (15, 16) were selected to undergo VEP, MR imaging, and MR spectroscopy (PEPSI). The project was approved by the University of Washington IRB Human Subjects Committee, and informed consent was obtained from all participants.

Expanded Disability Status Scale (EDSS)

Kurtzke's EDSS scale (17) was used for the clinical rating, which was based on neurologic examination performed under the direction of a neurologist.

Visual Evoked Potentials

Pattern reversal VEPs were recorded from the occiput to monocular stimulation with a full-field reversing checkerboard pattern. Each check subtended 30 minutes of arc at the observer's eye with a contrast exceeding 75%. The overall field subtended 16.4° of arc. Reversal rate was one per second. Recording electrodes were gold-plated cups affixed to abraded skin with conductive cream at locations Oz, O1, and O2, with reference at Fz (O is an abbreviation for occipital in the International Ten-Twenty System) (18, 19). These are the three scalp electrodes that are positioned over the occipital cortex on the back of the head (19). The analog signal was amplified and filtered with a bandpass of 30 to 500 Hz, digitized, and averaged with an analysis time of 200 milliseconds for 300 to 500 trials per average. The signals from the lateral leads were checked for lateralization of the response, but none was observed in this sample and thus all analyses were done with Oz signal. The first negativity (N75), first positivity (P100), and second negativity (N145) of the signals, recorded at Oz, were cursored and compared with normal values (literature norms plus small laboratory sample). Values for P100 that exceeded 117 milliseconds (105 milliseconds + 3 SD) were considered abnormal. Each subject had both right- and left-sided VEP measurements. Subjects were separated into groups on the basis of their VEP results. Subjects demonstrating abnormal VEPs on either the left or the right were placed in the abnormal VEP group. Subjects in the normal VEP group were normal on both sides. Nine MS subjects had abnormal VEPs and eight had normal VEPs. Several of the patients with abnormal VEPs had considerable asymmetry between the left and right eye stimulation response, but it was not consistently on the left or right side.

MR Imaging and MR Spectroscopy

MR imaging and MR spectroscopy (PEPSI) were performed on a 1.5-T Signa scanner using version 5.4 system software. The head coil was a custom-made, receive-only, short quadrature bird cage (20). It included 12 struts on a 19 × 22-cm elliptical cross section that extended 20 cm from a conductive endcap at the top to the head. Its shorter length and tighter coupling produces an approximately 40% better signal-to-noise ratio within the brain than does the standard, larger quadrature head coil supplied with the MR scanner. This radio frequency head coil, which has a square root signal-to-noise improvement over the conventional quadrature head coil, was used. Axial MR imaging parameters included contiguous dual-echo images, one echo with low CSF signal intensity (2000/35, TR/TE), one T2-weighted echo with high CSF signal intensity (2000/80), and a section thickness of 5 mm. The MR images were used to detect brain lesions, to define the anatomic location of the axial PEPSI section, and to calculate the CSF distribution map used for proton metabolite intensity correction. The section chosen for PEPSI was in the axial plane and passed through the mid-thalamus. The PEPSI pulse sequence consisted of three parts: interleaved water and spatial suppression, spin-echo excitation of the section of interest, and echo-planar spatial-spectral encoding with a series of periodically inverted readout gradients to simultaneously encode spectral information and one spatial domain, as described previously (21–23). The second spatial domain was encoded by conventional phase-encoding. PEPSI measurements were performed with the following parameters: 4000/272/4, a spatial matrix of 32 × 32 voxels, a field of view of 24 cm, a section thickness of 20 mm, a spectral width of 32 kHz, a frame size of 16,384 complex data points (32 spatial points convolved with 512 spectral points), acquisition of partial echoes to permit magnitude reconstruction, and an acquisition time of 9 minutes. A TE of 272 was chosen to obtain an in-phase doublet of lactate and to minimize residual peripheral lipid resonances. A separate PEPSI data set was obtained without water suppression for metabolite intensity normalization (2000/20). The raw time-domain data were sorted into a complex 3-D matrix (one dimension for spectral encoding and two dimensions of spatial encoding) for a 3-D Fourier transform. Spectral reconstruction was performed as reported previously (22, 23). A baseline correction was performed using the data points to the left of the water resonance. Metabolite maps were calculated from the spectral resonances of choline, creatine, NAA, and lactate by integrating spectral regions that extended 0.05 ppm to the left and right sides of each resonance. Metabolite maps were displayed and quantitated using NIH image 1.55 software. Regions of interest (ROIs) were defined on the conventional MR images for each subject.

Data Analysis

Twelve ROIs of the brain (Fig 1) were chosen in white matter tracts that covered a large portion of the optic radiations. The 12 brain regions were superimposed on T2-weighted MR images at the PEPSI section location, and each of the regions was evaluated visually for the presence of MS lesions. Each PEPSI image section was equivalent in brain location to four contiguous 5-mm-thick conventional MR images. Metabolite images were created for NAA, creatine, and choline. Each chemical image was normalized to a short-echo water PEPSI scan (no water suppression). Metabolite images were evaluated by averaging the intensities within a 1.5 × 1.5-cm ROI. Primary visual tracts from a computer-generated brain atlas were registered onto each subject's MR images using computer software that adjusted the pathways to fit various brain shapes and sizes. Abnormal brain regions were localized to the primary visual using a 3-D anatomic atlas. The atlas was registered to the patient's MR images using a 3-D algorithm that matched voxels in the corresponding volume showing high gradient magnitudes (24). This approach does not depend on related intervolume voxel intensities, and will converge in the presence of conflicting gradients caused by atlas structures and MS lesions. Registration errors over the entire volume were averaged, and conflicting regions were essentially ignored. This registration method compensates for variation in patient positioning or for imaging data that have unrelated voxel intensities as generated by different MR sequences. Figure 2 shows an example of a subject's MR images with the registered primary visual pathways. ROIs were placed in identical anatomic brain areas for all subjects. Reproducible placement of ROIs was achieved by superimposing MR image contours (brain perimeter, lateral ventricles, sulci, etc) onto the subject's metabolite image (Fig 3).

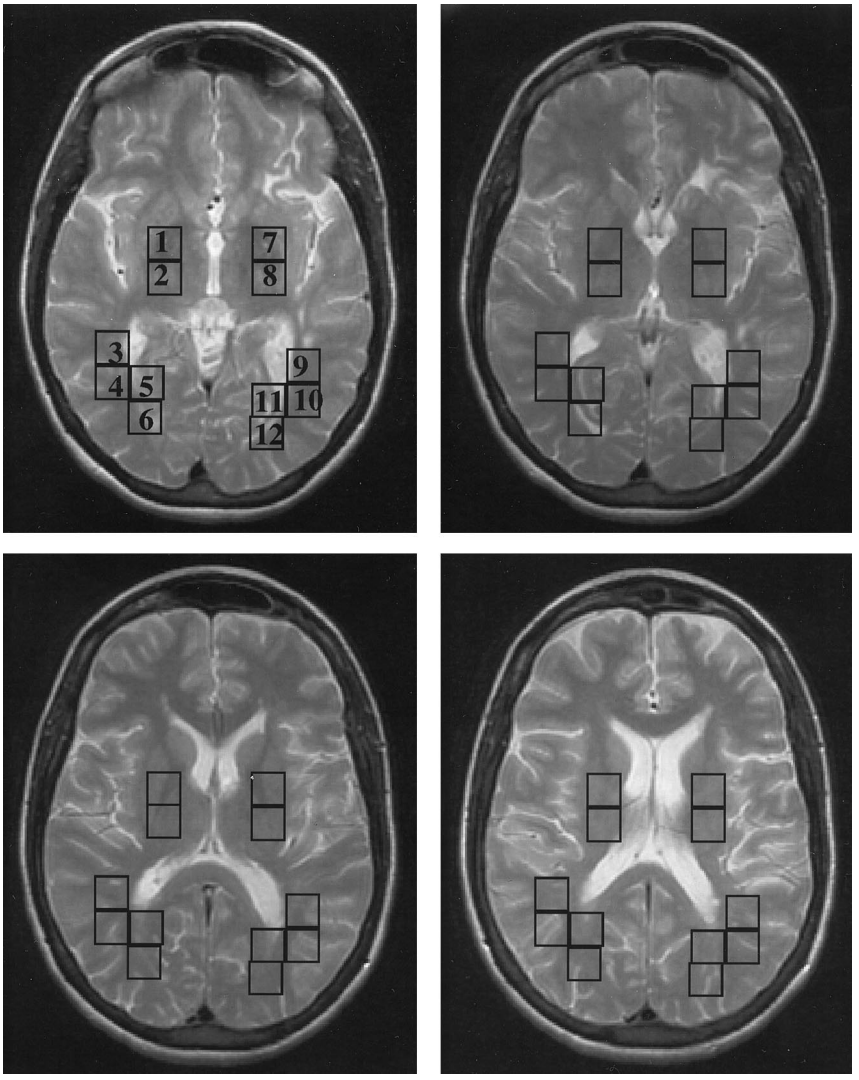

FIG 1. Four contiguous axial MR images (2000/80) from one MS patient. *Boxes* outline the anatomic ROIs for which proton spectroscopic image data were compared between MS subjects with normal and abnormal evoked potentials. The images are arranged from most inferior (*upper left*) to most superior (*lower right*).

CSF Correction and Spectral Intensity Normalization

The ROI metabolite intensity values were corrected for the amount of CSF that contributed to the 3-D ROI. The dual-echo MR images, represented in the spectroscopic section, were analyzed by using computer software to discriminate between CSF and the rest of the brain. Software was used to implement the following procedure for determining the number of CSF pixels within the brain: 1) the image pixel intensities from 10 MR image files (five double-echo sections surrounding the PEPSI section) were read into memory; 2) the intensities from all pixels between rows 65 to 200 and columns 81 to 180 for each image were averaged; 3) two intensity limits were set using the following equations: limit 1 = average of first-echo average × 1.1, limit 2 = average of second-echo average × 1.2; 4) the whole 256 × 256 image was searched for image intensities of the first-echo image with values less than limit 1 and for image intensities of the second-echo image greater than limit 2; 5) a new image was created with 0's for all pixels that did not meet the condition in step 4 and 1's for all pixels that met the condition; 6) the number of pixels determined to be CSF was counted for each image and used in the following equation to determine the percentage of brain within the ROI: brain fraction = 1 − (CSF pixels/total number of pixels in ROI); 7) the metabolite image intensity values were corrected by dividing the ROI average intensity by the brain fraction described above and by the ROI average intensity from the water PEPSI scan. Corrected intensity values were obtained for each ROI for the 17 MS subjects and plotted on scatter graphs along with normal and abnormal evoked potential responses. ROIs were also superimposed onto each patient's MR images to determine whether the ROI contained an area of MR-detectable lesions. This was done to ascertain whether spectral changes in the brain were associated with MR-detectable lesions in those same areas or whether the spectral changes were independent of lesion presence or absence as determined by MR imaging.

Statistics

For statistical analysis, the CSF-corrected, water-normalized, metabolite ROI values were placed into two groups: VEP normal or VEP abnormal. A *t*-test was performed to determine significant difference between the mean metabolite values for the two groups for each of the 12 ROIs. A probability value correction was made for the multiple *t*-tests that were performed on all the ROIs based on the probability of committing a type I error as described by Zar (25). The fraction of 12 ROIs with MR-detectable lesions was calculated for each subject and a *t*-test was performed comparing the MR imaging lesion fraction between the VEP abnormal and VEP normal groups. A *t*-test was also performed on the EDSS score comparing VEP abnormal and normal groups. Linear regression analysis was used to test the correlation between MR lesion fraction and NAA and also between MR lesion fraction and EDSS score.

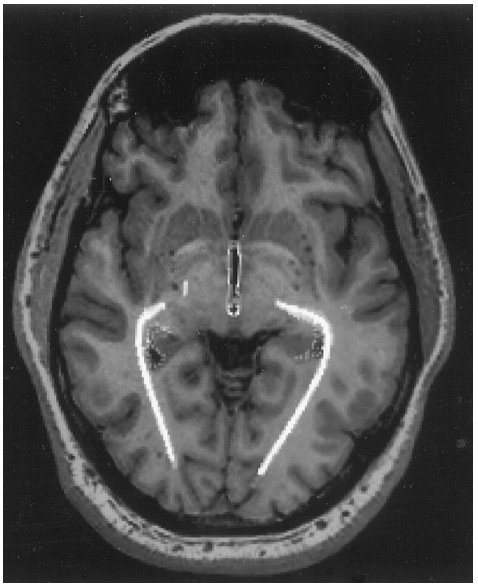

FIG 2. Registration of the optic radiations of the primary visual tracts from a computer anatomic atlas to an MR image of a patient with MS. An active contour model was used to obtain outer brain contours from the MR image and a corresponding section from the anatomic atlas. Principle moments of closed contours were used to determine a linear transformation, which was applied to align the two contours (outline of brain). The same transformation was then applied to interior atlas contours to register the visual pathways (shown in *white*).

Results

The Table shows the EDSS value, NAA value (averaged across the 12 ROIs), the MR-detectable lesion fraction, and the VEP type for each subject. On the basis of these data, the EDSS score was significantly higher in the abnormal VEP group than in the normal VEP group (t value 2.52, $df = 15$, $P < .05$). The average NAA value was significantly lower in the abnormal VEP group than in the normal VEP group (t value 4.52, $df = 15$, $P < .0005$). The MR-detectable lesion fraction was significantly higher in the abnormal VEP group than in the normal VEP group (t value 2.19, $df = 15$, $P < .05$). There was also a significant correlation between MR-detectable lesion fraction and EDSS score ($r = .58$, $P < .025$) and also between MR-detectable lesion fraction and NAA ($r = .55$, $P < .025$).

In the individual region analysis, the NAA was significantly lower in the abnormal VEP group than in the normal VEP group for four of 12 ROIs (Fig 4, top). Choline was significantly lower in the abnormal VEP group only in ROI 1 (Fig 4, middle). ROI 1 is located on the patient's right side basal ganglia area (Fig 1). Creatine was not statistically different in any of the 12 ROIs (Fig 4, bottom). A striking difference between the VEP abnormal and VEP normal groups can be observed in a graph of NAA normalized to

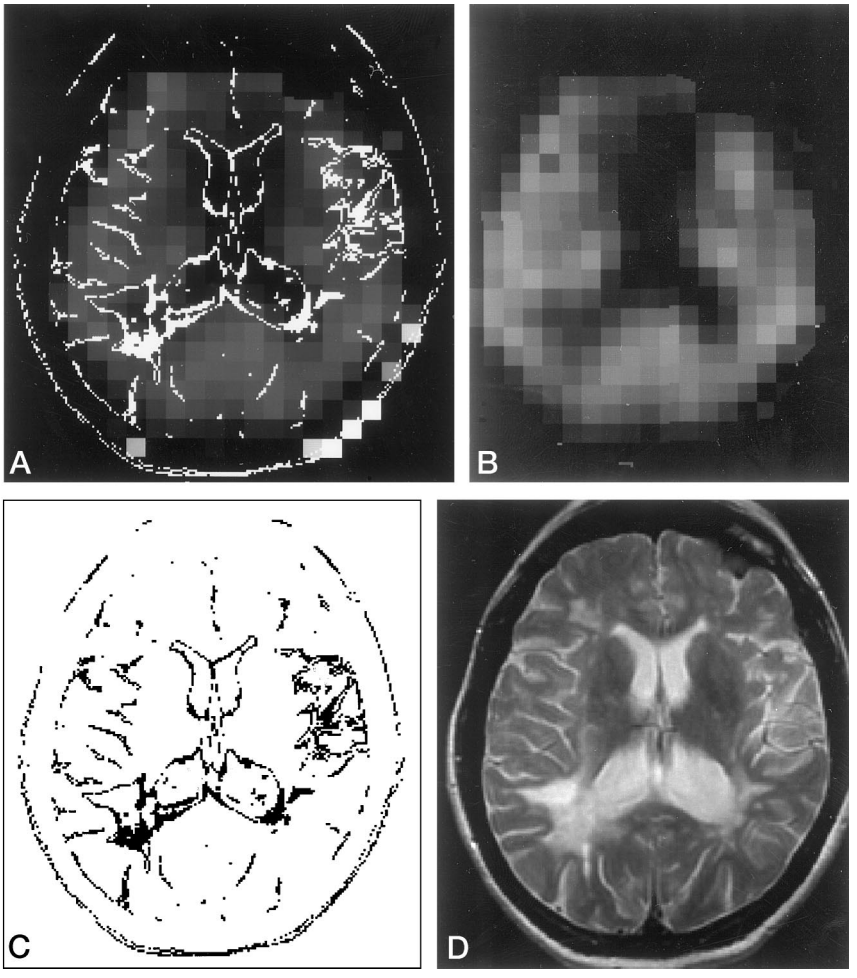

FIG 3. Set of images used to create the contour overlay onto spectroscopic image.

A, NAA image with contour overlay.

B, NAA PEPSI image.

C, Binarized conventional MR image using NIH image 1.55 software to create contour overlay. Thresholding was done to outline the lateral ventricles, several sulci including the sylvian fissure, and the outline of the scalp.

D, MR image (2000/80).

Expanded Disability Status Scale (EDSS) score, average NAA, and MR-detectable lesion fraction for MS patients with normal and abnormal visual evoked potentials (VEP)

Normal VEP Group			
Subject	EDSS Score	Average NAA*	Lesion Fraction†
1	0.0	7116	0.00
2	1.0	8246	0.42
3	1.0	7979	0.17
4	2.0	8452	0.08
5	2.5	8307	0.42
6	2.5	6933	0.67
7	3.0	7537	0.25
8	4.0	6972	0.58
Mean ± SD	2.0 ± 1.3	7692 ± 632	0.32 ± 0.24
Abnormal VEP Group			
Subject	EDSS Score	Average NAA*	Lesion Fraction†
1	1.0	7508	0.17
2	2.0	6028	0.92
3	3.0	5754	0.50
4	3.0	4887	0.50
5	3.5	6803	0.75
6	6.0	6396	0.67
7	6.5	6194	0.17
8	7.5	5573	1.00
9	7.5	6341	0.92
Mean ± SD	4.4 ± 2.5	6164 ± 747	0.62 ± 0.31
t values‡	2.52	4.52	2.19

* Average NAA value from all 12 ROIs

† Fraction of the 12 ROIs with MR-detectable lesions

‡ *t* values were calculated by performing a *t*-test comparing the abnormal VEP group with the normal VEP group.

water for ROI 3 (Fig 5). ROI 3 showed the greatest significant difference between the two groups (*t* value 4.5, $P < .001$).

Figure 6 shows MR image data, PEPSI-NAA images, and PEPSI spectra from two typical MS patients, one from the VEP normal group and one from the VEP abnormal group. Both MR images show detectable lesions within some of the ROIs illustrated in Figure 1. The patient with abnormal VEPs had more extensive MR-detectable lesions and lower NAA levels than did the patient with normal VEPs. The NAA images (Fig 6C and D) and spectra (Fig 6E) demonstrate low NAA in the right posterior periventricular white matter region for the patient with abnormal VEPs. Although the EDSS scores differed by only one unit between these two patients (Fig 6), there was a 36% difference in NAA levels. Also, there was a change in concentration of NAA in the patient with abnormal VEP going from the top-left spectrum to the bottom-right spectrum of Figure 6E. For the spectra from the patient with abnormal VEP, the NAA levels are lower in the spectra in rows 1 and 2 (inside the visual tract) of Figure 6E relative to row 3, which is outside the visual tract. For the subject with the abnormal VEP in Figure 6, the entire ROI is abnormal on MR imaging and appears to be more sensitive than NAA; however, NAA had a much more significant *t* value than MR imaging with the *t*-test comparison between abnormal and normal VEP groups.

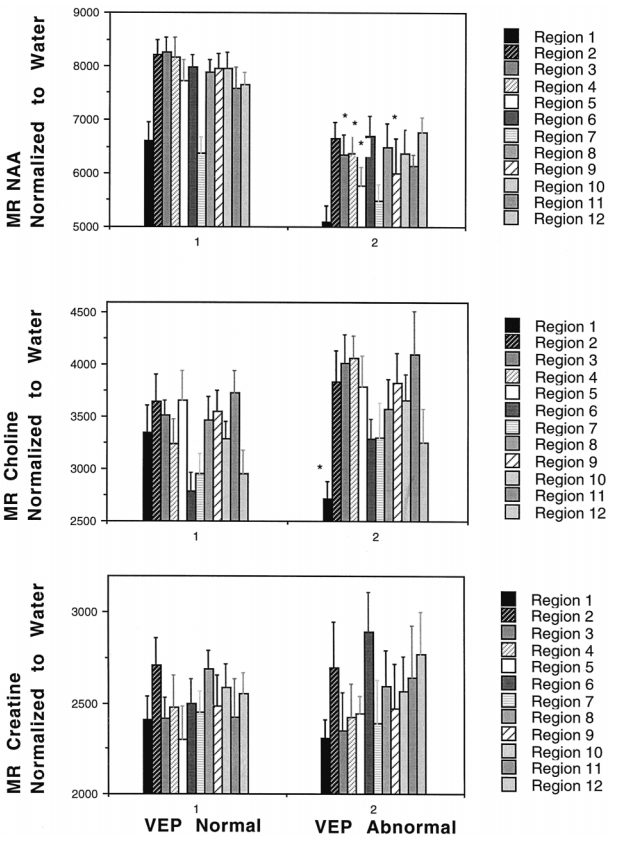

FIG 4. Bar plots of MR NAA (*top*), choline (*middle*), and creatine (*bottom*) for normal and abnormal VEP groups. Data from all 12 ROIs are given for each plot (locations are shown in Fig 1). Error bars are the standard error of the mean. Regions marked with an *asterisk* in VEP abnormal group were significantly different ($P < .01$) from those in VEP normal group.

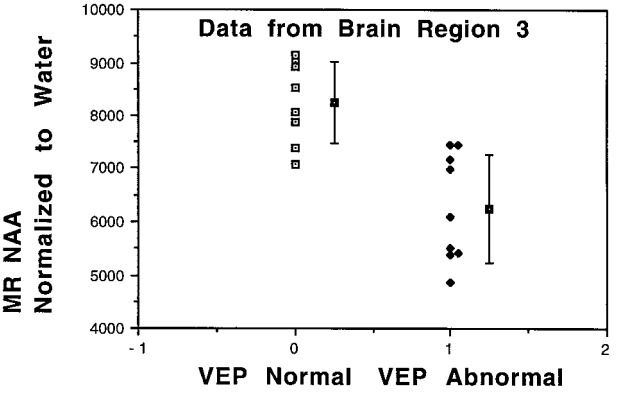

FIG 5. Scatter plot of MR NAA normalized to water (CSF-corrected) for normal and abnormal VEP groups for ROI 3 shown in Figure 1. The average (error bars are the standard deviation) for each group is also displayed to the right of the scatter plot. Note that NAA values in the abnormal VEP group are generally lower than those in the normal VEP group.

Discussion

The main result of this study is that the MR spectroscopic NAA values within the visual pathways were significantly decreased in MS subjects with abnormal VEPs as compared with those in MS subjects with normal VEPs. NAA showed the most significant

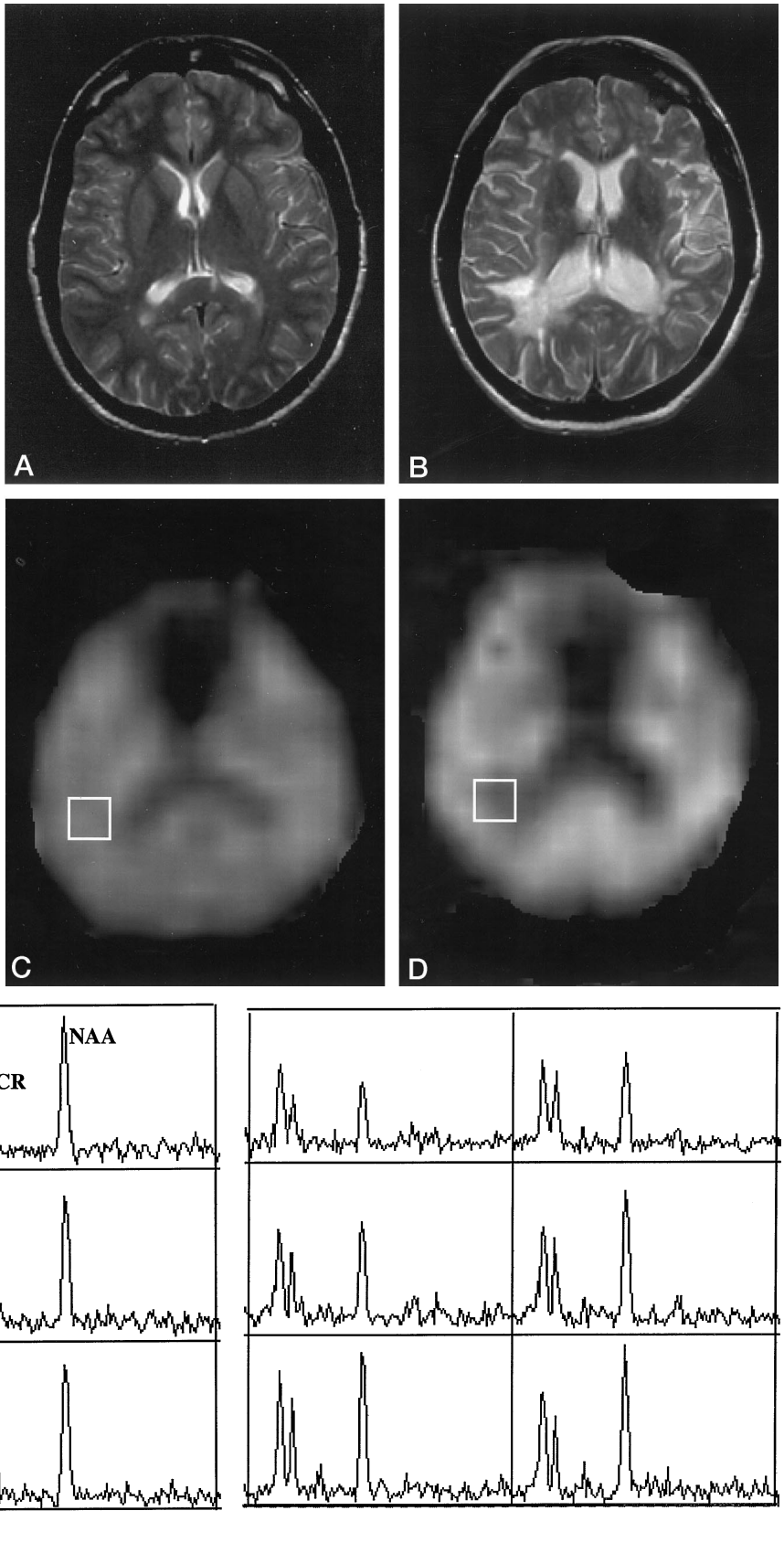

FIG 6. *A* and *B*, MR images (2000/85) from MS patients with normal (*A*) and abnormal (*B*) VEP.

C and *D*, PEPSI-NAA metabolite images (4000/272; matrix, 32 × 32; section thickness, 20 mm; field of view, 20 cm) from MS patients with normal (*C*) and abnormal (*D*) VEPs. Note that in *D*, NAA has decreased signal intensity in right posterior periventricular area. In *C*, NAA value in *box* is 8511 and EDSS score is 1.0; in *D*, NAA value in *box* is 5417 and EDSS score is 2.0.

E, PEPSI spectra from the right posterior periventricular area in the same patient with normal VEP (*left*) and the same patient with abnormal VEP (*right*). Note the decreased NAA level in the spectrum in the upper left of the abnormal VEP spectral set (*right*). The spectra from rows 1 and 2 came from the brain region shown by the *boxes* in *C* and *D*, which is within the visual tract. The spectra from row 3 came from adjacent regions next to the *boxes* but outside the visual tract.

change (greatest *t* value) between VEP groups relative to all the other parameters measured, including MR-choline, MR-creatine, EDSS score, and MR-detectable lesion fraction. NAA is a specific marker for neuronal damage, because NAA is not normally found in mature glial cells (26, 27). A decrease in NAA has been attributed to axonal loss (9), active degradation of NAA in injured neurons (28), and gliosis (12). MS is thought to be a disease of myelin rather than of neurons. However, these data show evidence that neuronal damage is involved in MS, as evidenced by the decrease in NAA. Nerve conduction slowing can be caused by demyelination (29), in which the axonal membrane reorganizes to allow continued conduction but at a slower rate. The physiological association between NAA and nerve conduction slowing may be explained by the metabolic relationship between glial cells (myelin) and neurons. The axon needs a very well-regulated microenvironment to maintain its normal biological state. It is understandable that demyelination may profoundly alter the biochemical state of the axon (30).

We have shown an association between NAA (measured from MR spectroscopy) and VEPs. In addition, associations between MR imaging and evoked potentials have also been reported in the literature (31–33). Filippi et al (31) demonstrated that the total amount of MR lesions and their distribution are related to multimodal evoked potentials and disability in MS patients. Levine et al (32, 33) showed correlations between brain stem auditory evoked potentials and the presence of MR-detectable MS lesions. This group also concluded that interaural time discrimination was closely related to brain stem auditory evoked potentials, and their data constitute some of the most direct evidence of a relationship between auditory performance, evoked potentials, and anatomy (as measured by MR-detectable lesions) (32). Our data provide evidence that there is a relationship between physiological function and biochemistry of the neuron (NAA).

These results indicate that a decrease in NAA levels may be important for normal electrophysiological functioning of the CNS. The decrease in NAA may be a contributing factor to the abnormal functioning of the visual system, and therapies that attempt to restore NAA to normal levels may help MS patients. Regardless of whether the deficit in NAA levels actually contribute to abnormal electrophysiological function or is merely associated with the abnormal function, the NAA levels could be used to monitor disease progression during a clinical trial to test new treatments for MS.

Conclusion

PEPSI is a technique that can be used to analyze chemical changes in multiple areas of the brain that may lie in or around known visual pathways. These chemical abnormalities in the visual white matter tracts may be related to defects measured with VEPs. NAA measured with PEPSI was more sensitive to VEP abnormalities than choline, creatine, MR-detectable lesions, or EDSS score.

Acknowledgments

We thank the technicians who acquired the evoked potential data (Dee Spellman, Mark Klein, and Roxane Hoon) and the MR technicians (Vern Terry and Denise Echelard). We also thank Jane Johnson for help with the preparation of the manuscript.

References

1. Paty DW. **Multiple sclerosis with an emphasis on MR imaging.** *Curr Neurol* 1991;11:169–198
2. Brusa A, Mortimer C, Jones SJ. **Clinical evaluation of VEPs to interleaved checkerboard reversal stimulation of central, hemi- and peripheral fields.** *Electroencephalogr Clin Neurophysiol* 1995;96:485–494
3. Bodis-Wollner I. **Sensory evoked potentials: PERG, VEP, and SEP.** *Curr Opin Neurol Neurosurg* 1992;5:716–726
4. Brasil-Neto JP. **Evoked potentials in multiple sclerosis: recent experience at the Locomotor System Diseases Hospital.** *Arq Neuropsiquiatr* 1991;49:204–207
5. Fulgente T, Thomas A, Lobefalo L, et al. **Are VEP abnormalities in optic neuritis (ON) dependent on plaque size? A reappraisal of the physiopathology of ON based on improved MRI and multiple-lead recordings.** *Ital J Neurol Sci* 1996;17:43–54
6. Jones SJ. **Visual evoked potentials after optic neuritis: effect of time interval, age and disease dissemination.** *J Neurol* 1993;240:489–494
7. van Diemen HA, Lanting P, Koetsier JC, Strijers RL, van WHK, Polman CH. **Evaluation of the visual system in multiple sclerosis: a comparative study of diagnostic tests.** *Clin Neurol Neurosurg* 1992;94:191–195
8. Arnold DL, Matthews PM, Francis G, Antel J. **Proton magnetic resonance spectroscopy of human brain in vivo in the evaluation of multiple sclerosis: assessment of the load of disease.** *Magn Reson Med* 1990;14:154–159
9. Matthews PM, Francis G, Antel J, Arnold DL. **Proton magnetic resonance spectroscopy for metabolic characterization of plaques in multiple sclerosis [published erratum appears in *Neurology* 1991;41:1828].** *Neurology* 1991;41:1251–1256
10. Narayana PA, Wolinsky JS, Jackson EF, McCarthy M. **Proton MR spectroscopy of gadolinium-enhanced multiple sclerosis plaques.** *J Magn Reson Imaging* 1992;2:263–270
11. Miller DH, Austin SJ, Connelly A, Youl BD, Gadian DG, McDonald WI. **Proton magnetic resonance spectroscopy of an acute and chronic lesion in multiple sclerosis.** *Lancet* 1991;337:58–59
12. van Hecke P, Marchal G, Johannik K, et al. **Human brain proton localized NMR spectroscopy in multiple sclerosis.** *Magn Reson Med* 1991;18:199–206
13. Grossman RI, Lenkinski RE, Ramer KN, Gonzalez SF, Cohen JA. **MR proton spectroscopy in multiple sclerosis.** *AJNR Am J Neuroradiol* 1992;13:1535–1543
14. Weinstein GW, Odom JV, Cavender S. **Visually evoked potentials and electroretinography in neurologic evaluation.** *Neurol Clin* 1991; 9:225–242
15. Poser C, Paty D, Scheinberg L, et al. **New diagnostic criteria for multiple sclerosis: guidelines for research protocols.** *Ann Neurol* 1983;1983:227–231
16. Peters AR, Geelen JAG, denBoer JA, Prevo RL, Minderhoud JM, Gravenmade EJ. **A study of multiple sclerosis patients with magnetic resonance spectroscopic imaging.** *Multiple Sclerosis* 1995;1:25–31
17. Kurtzke JF. **Rating neurologic impairment in multiple sclerosis: an expanded disability status scale (EDSS).** *Neurology* 1983;33:1444–1452
18. Lewine JD, Orrison WW. **Clinical electroencephalography and event-related potentials.** In: Orrison WW, Lewine JD, Sanders JA, Hartshorne MF. eds. *Functional Brain Imaging.* St Louis: Mosby; 1995:327–368
19. Jasper HH. **Report of the committee on methods of clinical examination in EEG. Appendix: the ten-twenty electrode system of the International Federation.** *Electroencephalogr Clin Neurophysiol* 1958;10:371–375

20. Hayes CE, Mathis CM. **Improved brain coil for fMRI and high resolution imaging.** In: *Proceedings of the Fourth Annual Meeting of the Society of Magnetic Resonance.* Society of Magnetic Resonance, Berkeley, CA; 1996:1414
21. Posse S, DeCarli C, LeBihan D. **Three-dimensional echo-planar MR spectroscopic imaging at short echo times in the human brain.** *Radiology* 1994;192:733–738
22. Posse S, Tedeschi G, Risinger R, Ogg R, Le BD. **High speed 1H spectroscopic imaging in human brain by echo planar spatial-spectral encoding.** *Magn Reson Med* 1995;33:34–40
23. Posse S, Dager SR, Richards TL, et al. **In vivo measurement of regional brain metabolic response to hyperventilation using magnetic resonance proton echo planar spectroscopic imaging (PEPSI).** *Magn Reson Med* 1997;37:858–865
24. Ostuni JL, Levin RL, Frank JA, DeCarli C. **Correspondence of closest gradient voxels: a robust registration algorithm.** *J Magn Reson Imaging* 1997;7:410–415
25. Zar JH. ***Biostatistical Analysis***. Englewood Cliffs, NJ: Prentice-Hall; 1984:162–205
26. Birken DL, Oldendorf WH. **N-acetyl-L-aspartic acid: a literature review of a compound prominent in 1H-NMR spectroscopic studies of brain.** *Neurosci Biobehav Rev* 1989;13:23–31
27. Gill SS, Small RK, Thomas DGT, et al. **Brain metabolites as 1H NMR markers of neuronal and glial disorders.** *NMR Biomed* 1989; 2:196–200
28. Bruhn H, Frahm J, Gyngell ML, Merboldt KD, Hanicke W, Sauter R. **Cerebral metabolism in man after acute stroke: new observations using localized proton NMR spectroscopy.** *Magn Reson Med* 1989;9:126–131
29. Waxman SG, Ritchie JM. **Molecular dissection of the myelinated axon.** *Ann Neurol* 1993;33:121–136
30. Huszak I. **Biochemical aspects of multiple sclerosis.** In: Lajtha A, ed. *Handbook of Neurochemistry, VII: pathological chemistry of the nervous system.* New York: Plenum Press; 1972:47–91
31. Filippi M, Campi A, Mammi S, et al. **Brain magnetic resonance imaging and multimodal evoked potentials in benign and secondary progressive multiple sclerosis.** *J Neurol Neurosurg Psychiatry* 1995;58:31–37
32. Levine RA, Gardner JC, Stufflebeam SM, et al. **Binaural auditory processing in multiple sclerosis subjects.** *Hear Res* 1993;68:59–72
33. Levine RA, Gardner JC, Fullerton BC, et al. **Effects of multiple sclerosis brainstem lesions on sound lateralization and brainstem auditory evoked potentials.** *Hear Res* 1993;68:73–88

Please see the Editorial on page 1002 in this issue.